LETTER

doi:10.1038/nature10508

ATM controls meiotic double-strand-break formation

Julian Lange[1], Jing Pan[1]†, Francesca Cole[2], Michael P. Thelen[3], Maria Jasin[2] & Scott Keeney[1,4]

In many organisms, developmentally programmed double-strand breaks (DSBs) formed by the SPO11 transesterase initiate meiotic recombination, which promotes pairing and segregation of homologous chromosomes[1]. Because every chromosome must receive a minimum number of DSBs, attention has focused on factors that support DSB formation[2]. However, improperly repaired DSBs can cause meiotic arrest or mutation[3,4]; thus, having too many DSBs is probably as deleterious as having too few. Only a small fraction of SPO11 protein ever makes a DSB in yeast or mouse[5] and SPO11 and its accessory factors remain abundant long after most DSB formation ceases[1], implying the existence of mechanisms that restrain SPO11 activity to limit DSB numbers. Here we report that the number of meiotic DSBs in mouse is controlled by ATM, a kinase activated by DNA damage to trigger checkpoint signalling and promote DSB repair. Levels of SPO11–oligonucleotide complexes, by-products of meiotic DSB formation, are elevated at least tenfold in spermatocytes lacking ATM. Moreover, *Atm* mutation renders SPO11–oligonucleotide levels sensitive to genetic manipulations that modulate SPO11 protein levels. We propose that ATM restrains SPO11 via a negative feedback loop in which kinase activation by DSBs suppresses further DSB formation. Our findings explain previously puzzling phenotypes of *Atm*-null mice and provide a molecular basis for the gonadal dysgenesis observed in ataxia telangiectasia, the human syndrome caused by ATM deficiency.

SPO11 creates DSBs via a covalent protein–DNA intermediate that is endonucleolytically cleaved to release SPO11 attached to a short oligonucleotide, freeing DSB ends for further processing and recombination[5] (Fig. 1a). SPO11–oligonucleotide complexes are a quantitative by-product of DSB formation that can be exploited to study DSB number and distribution[5–7] (Supplementary Fig. 1). We examined SPO11–oligonucleotide complexes by SPO11 immunoprecipitation and 3′-end labelling of whole-testis extracts from $Atm^{-/-}$ mutant mice, which have multiple catastrophic meiotic defects, including chromosome synapsis failure and apoptosis[8–12]. The $Atm^{-/-}$ phenotype resembles that of mutants lacking DSB repair factors such as DMC1, indicating that absence of ATM causes meiotic recombination defects. Although $Spo11^{-/-}$ mutation is epistatic to $Atm^{-/-}$ (refs 11, 12), the functional relationship between ATM and SPO11 is complex, as meiotic defects of $Atm^{-/-}$ mice are substantially rescued by reducing *Spo11* gene dosage[13,14] (discussed later).

Unexpectedly, we found that adult $Atm^{-/-}$ testes exhibited an approximately tenfold elevation in steady-state levels of SPO11–oligonucleotide complexes relative to wild-type littermates (Fig. 1b) (11.3 ± 4.5-fold, mean and standard deviation, $n = 7$ littermate pairs). This finding contrasts with $Dmc1^{-/-}$ testes, which showed a ~50% reduction in SPO11–oligonucleotide complexes (0.51 ± 0.06-fold relative to wild type, $n = 5$) (Fig. 1c), as previously shown[5,7]. The mutants share similar arrest points in prophase I, as determined by molecular and histological data[12]; thus, increased SPO11–oligonucleotide complexes in $Atm^{-/-}$ spermatocytes are not an indirect consequence of arrest or of an increased fraction of meiocytes harbouring such complexes.

In $Atm^{-/-}$ testes, levels of free SPO11 (that is, not bound to an oligonucleotide) were much lower than in wild type (Fig. 1b). This is not because a large fraction of SPO11 has been consumed in covalent complexes with DNA—which alters its electrophoretic mobility—as free SPO11 was not restored to wild-type levels by nuclease treatment (Fig. 1d). Instead, because *Spo11* transcript levels in wild type are highest in later stages of meiotic prophase[15–18], after the arrest point of $Atm^{-/-}$ cells, reduced free SPO11 is attributable to the lack of later meiotic cell types, consistent with the reduced free SPO11 also found in

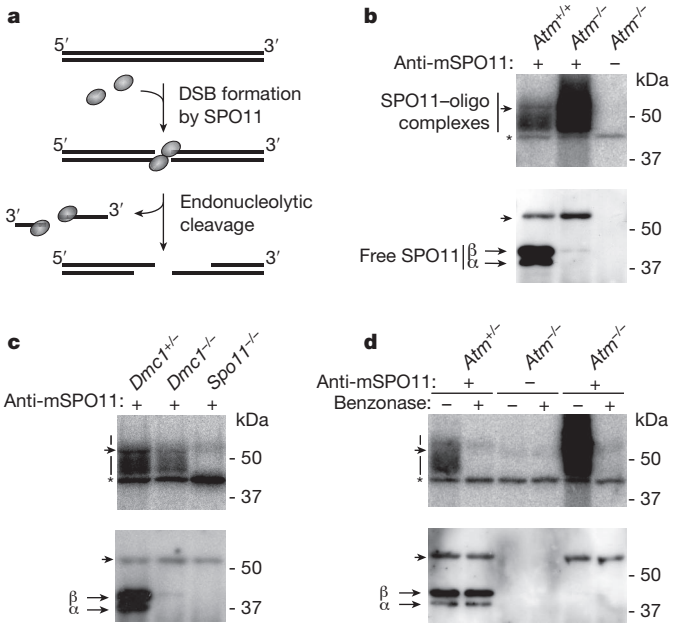

Figure 1 | SPO11 activity and expression in the absence of ATM. **a**, SPO11 attacks the DNA phosphodiester backbone, forming a covalent intermediate with the 5′ strand termini of the DSB. Endonucleolytic cleavage removes SPO11 covalently attached to an oligonucleotide. **b**, **c**, Steady-state levels of SPO11–oligonucleotide (SPO11–oligo) complexes are elevated in $Atm^{-/-}$ testes (**b**), but are decreased in $Dmc1^{-/-}$ testes (**c**). Anti-mSPO11, anti-mouse SPO11 antibody. SPO11 immunoprecipitates from extracts of whole adult testes were treated with terminal transferase and [α-^{32}P] dCTP, resolved by SDS–PAGE, and transferred to a membrane. Representative experiments using littermates of the indicated genotypes are shown. Top, autoradiograph. Bottom, anti-SPO11 western blot detection. Vertical lines, extent of SPO11-specific signals; α and β, major SPO11 isoforms; asterisk, non-specific terminal transferase labelling; arrowheads, migration position of immunoglobulin heavy chain. **d**, Treatment of labelled SPO11 immunoprecipitates with benzonase does not detectably alter levels of free SPO11, but this sequence non-specific nuclease efficiently removes the 3′-end label (compare lanes ± benzonase), and was previously shown to completely remove DNA covalently bound to yeast Spo11 (ref. 1).

[1]Molecular Biology Program, Memorial Sloan-Kettering Cancer Center, 1275 York Avenue, New York, New York 10065, USA. [2]Developmental Biology Program, Memorial Sloan-Kettering Cancer Center, 1275 York Avenue, New York, New York 10065, USA. [3]Physical and Life Sciences Directorate, Lawrence Livermore National Laboratory, Livermore, California 94550, USA. [4]Howard Hughes Medical Institute, Memorial Sloan-Kettering Cancer Center, 1275 York Avenue, New York, New York 10065, USA. †Present address: Cell Biology Department, University of Texas Southwestern Medical Center, Dallas, Texas 75390, USA.

Dmc1$^{-/-}$ cells (Fig. 1c). As expected, the residual SPO11 protein in *Atm*$^{-/-}$, like *Dmc1*$^{-/-}$, testes was mostly SPO11β (Fig. 1b, c). SPO11α and SPO11β are major protein isoforms encoded by developmentally regulated splice variants; SPO11β is expressed earlier and is sufficient for nearly normal DSB levels[5,15,17–20].

Elevated SPO11–oligonucleotide complexes can be explained by an increased number of meiotic DSBs and/or a longer lifespan of complexes. To distinguish between these possibilities, we examined the initial appearance and persistence of SPO11–oligonucleotide complexes in juvenile mice, in which the first suite of spermatogenic cells proceeds through meiosis in a semi-synchronous fashion[21]. First, we assayed SPO11–oligonucleotide complexes in whole-testis extracts from wild-type C57BL/6J mice at postnatal days (d)7 to 24 (Fig. 2a). SPO11–oligonucleotide complexes first appeared between d9 and d10, when most cells of the initial cohort had entered leptonema. SPO11–oligonucleotide complexes persisted or increased slightly until d15, when the first cohort had progressed into pachynema. Levels rose still further from d16 to d18, coincident with the second cohort of spermatogenic cells reaching leptonema[21]. Thus, SPO11–oligonucleotide complexes appear at the same time as cell types that experience the majority of meiotic DSBs. Consistent with findings in mutants (see earlier), only trace amounts of free SPO11 protein were seen when SPO11–oligonucleotide complexes first appeared, with SPO11β the predominant isoform at these times (Fig. 2a). Importantly, SPO11–oligonucleotide complex levels did not decline between the first and second spermatogenic cohorts. We infer that the lifespan of the complexes is long relative to the duration of prophase, and that an increased lifespan is not a likely explanation for the large increase in steady-state SPO11–oligonucleotides in adult *Atm*$^{-/-}$ testes.

In support of this interpretation, we found that SPO11–oligonucleotide complexes were undetectable in *Atm*$^{-/-}$ testes at d7 (data not shown) but were already elevated 3.3-fold compared with a wild-type littermate when they first appeared, increasing to 8.4-fold over wild type by d12 (Fig. 2b). Because *Atm*$^{-/-}$ juveniles showed higher SPO11–oligonucleotide levels as soon as the first leptotene cells appeared, we conclude that most, if not all, of the increase reflects a greater number of meiotic DSBs occurring during prophase I.

Meiotic defects of mice lacking ATM are substantially suppressed by reducing *Spo11* gene dosage: *Spo11*$^{+/-}$ *Atm*$^{-/-}$ spermatocytes pair and recombine their autosomes and progress through meiotic prophase to metaphase I, where they arrest due to a failure in sex chromosome pairing and recombination[13,14]. The reason for this puzzling rescue was unknown, but our current findings suggest an explanation: the majority of meiotic defects in *Atm*-null spermatocytes are caused by grossly elevated DSB levels, which are lowered by *Spo11* heterozygosity (which reduces SPO11 protein levels by half in adult and juvenile testes (ref. 17 and our unpublished data)). Indeed, we found SPO11–oligonucleotide complexes in *Spo11*$^{+/-}$ *Atm*$^{-/-}$ mice to be substantially reduced compared with *Atm*$^{-/-}$ littermates (Fig. 3a). The remaining increase in SPO11–oligonucleotide complexes in *Spo11*$^{+/-}$ *Atm*$^{-/-}$ mutants compared with wild type (range of 4.5- to 7.8-fold, $n = 2$) is not simply a consequence of metaphase arrest, because SPO11–oligonucleotide complexes were not elevated in mice that exhibit a similar arrest point due to absence of MLH1, a protein involved late in recombination[22] (Fig. 3a). The fact that DSBs are still elevated in *Spo11*$^{+/-}$ *Atm*$^{-/-}$ spermatocytes relative to wild type may account for some or all of the remaining defects in this mutant, including axis interruptions at sites of ongoing recombination and persistent unrepaired DSBs late in prophase I (ref. 14).

Our findings indicate that the absence of ATM renders the extent of DSB formation sensitive to SPO11 expression levels. Therefore, we reasoned that increasing SPO11 expression should further elevate DSB formation in ATM-deficient cells. To test this prediction, we used a previously described transgene (*Xmr-Spo11β*$_B$) that expresses the SPO11β isoform[18]. Indeed, there was substantial further elevation of SPO11–oligonucleotide complex levels (20.9 ± 1.5-fold over wild-type littermates, $n = 3$) upon introduction of this transgene in an *Atm*-null background with intact endogenous *Spo11* (Fig. 3b). By contrast, the transgene resulted in only a modest increase in SPO11–oligonucleotide complexes in an ATM-proficient background (1.1 ± 0.05-fold, $n = 3$) (Fig. 3b).

SPO11–oligonucleotide complexes from *Atm*-null testes were consistently shifted to a higher electrophoretic mobility compared to wild type or other mutants (Figs 1, 2b and 3). To examine the distribution of

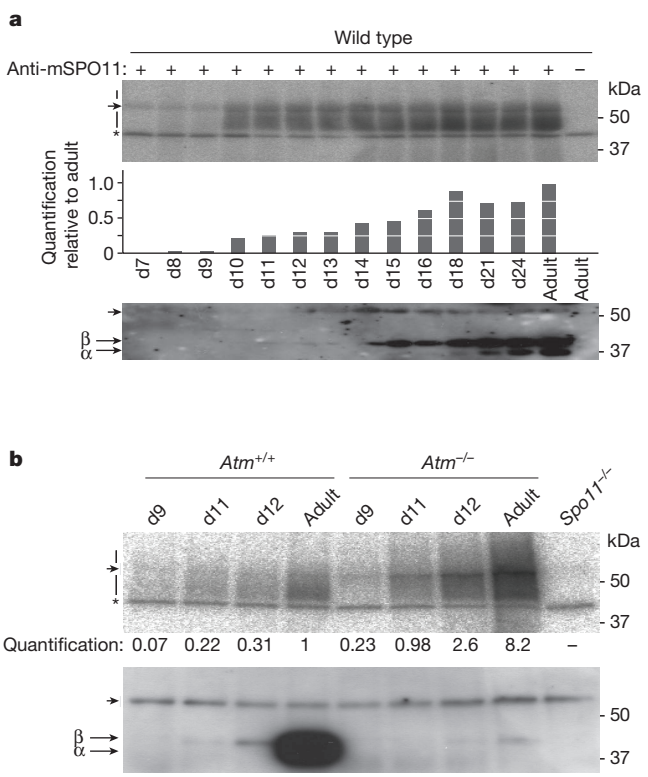

Figure 2 | SPO11–oligonucleotide complexes from juvenile mice. **a**, SPO11–oligonucleotide complexes from testes of wild-type mice from d7–d24. Top, autoradiograph. Middle, quantification. Bottom, anti-SPO11 western detection. **b**, SPO11–oligonucleotides are elevated in testes from juvenile *Atm*$^{-/-}$ mice. Top, autoradiograph. Bottom, anti-SPO11 western detection.

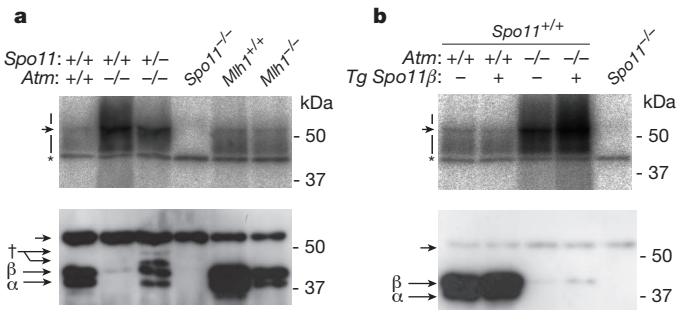

Figure 3 | *Spo11* gene dosage modulates SPO11–oligonucleotide complex levels in *Atm*-deficient spermatocytes. **a**, SPO11–oligonucleotide complexes are reduced in *Spo11*$^{+/-}$ *Atm*$^{-/-}$ testes relative to *Atm*$^{-/-}$, but are more abundant than in wild type or in an *Mlh1*$^{-/-}$ mutant, which similarly arrests at metaphase. Consistent with further meiotic progression than *Atm*$^{-/-}$, both SPO11 isoforms (α and β) are expressed in *Spo11*$^{+/-}$ *Atm*$^{-/-}$ testes, although at reduced levels due to *Spo11* heterozygosity. Dagger, lower-mobility polypeptides probably originating from the *Spo11* knockout allele[18]. **b**, SPO11–oligonucleotide complexes are further elevated by SPO11β expression from the *Xmr-Spo11β*$_B$ transgene (*Tg Spo11β*)[18] in *Atm*$^{-/-}$ spermatocytes. Introducing this transgene into an otherwise wild-type background only modestly increased SPO11–oligonucleotide complex levels.

oligonucleotide lengths, labelled complexes were protease-digested and the resulting oligonucleotides were electrophoresed on a high-resolution gel (Fig. 4a). As previously shown[5], SPO11–oligonucleotides from wild type have a bimodal length distribution with prominent subpopulations at apparent sizes of ~15–27 and ~31–35 nucleotides. $Atm^{-/-}$ mice showed a different pattern with or without the *Spo11* transgene: oligonucleotides in the shorter size range were less abundant relative to the ~31–35 nucleotide class and longer oligonucleotides appeared, including an abundant class of ~40–70 nucleotides and a subpopulation that ranged to >300 nucleotides. $Spo11^{+/-}$ $Atm^{-/-}$ mice showed an intermediate pattern, with more pronounced enrichment of the ~31–35 nucleotide class relative to both smaller and longer oligonucleotides. These results indicate that ATM influences an early step in nucleolytic processing of meiotic DSBs, as has been proposed in yeast[23]. In principle, altered oligonucleotide sizes could reflect changes in preferred positions of the endonucleolytic cleavage that releases the SPO11–oligonucleotide complex, effects on 3′→5′ exonucleolytic digestion of SPO11–oligonucleotides after they are formed, or occurrence of SPO11-induced DSBs at adjacent positions on the same DNA duplex (M. Neale, personal communication). Resection defects and adjacent DSBs (which conventional cytology would be unable to resolve) are both possible explanations for why SPO11–oligonucleotide complexes in $Atm^{-/-}$ spermatocytes show a greater increase than RAD51 focus numbers[14].

Our results reveal an essential but previously unsuspected function for ATM in controlling the number of SPO11-generated DSBs. We suggest that activation of ATM by DSBs triggers a negative feedback loop that leads to inhibition of further DSB formation (Fig. 4b) via phosphorylation of SPO11 or its accessory proteins, several of which are known to be phosphorylated in budding yeast (for example, ref. 24) and are conserved in mammals[2]. ATM is activated in the vicinity of DSBs, as judged by SPO11- and ATM-dependent appearance of γH2AX (phosphorylated histone variant H2AX) on chromosomes at leptonema[12,13,25]. Thus, we envision that the negative feedback loop operates at least in part at a local level, perhaps discouraging additional DSBs from forming close to where a DSB has already formed. Such a mechanism could minimize instances where both sister chromatids are cut in the same region, and could also promote more even spacing of DSBs along chromosomes. These studies provide a new molecular framework for understanding the gonadal phenotypes of patients with ataxia telangiectasia[26], which is caused by ATM deficiency[27].

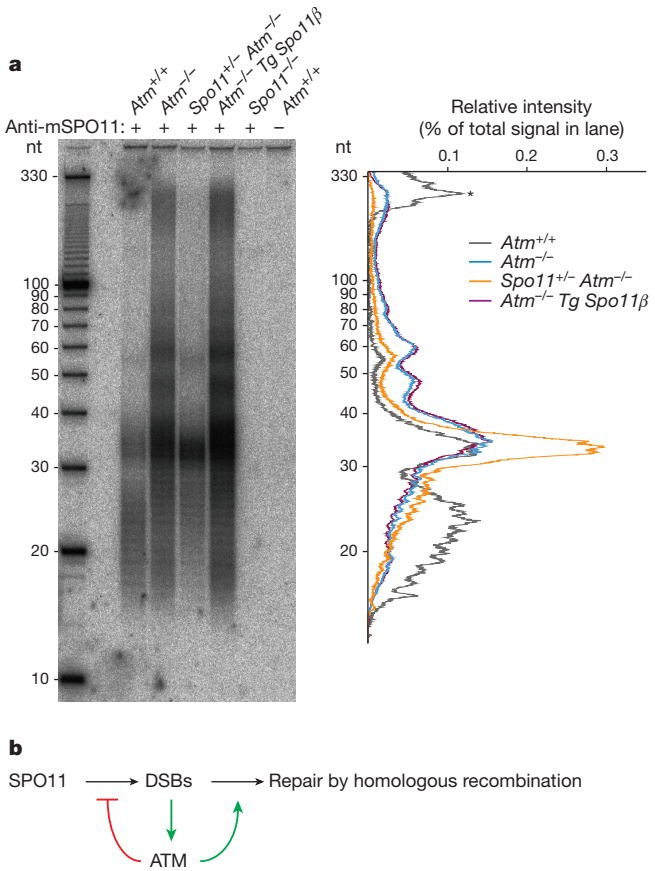

Figure 4 | Roles of ATM in DSB formation and processing. **a**, SPO11–oligonucleotide length distribution is altered in $Atm^{-/-}$ spermatocytes. End-labelled SPO11–oligonucleotide complexes were treated with protease to digest the bound protein before electrophoresis on denaturing PAGE. Left, autoradiograph. Right, background-subtracted lane traces normalized to total signal within each lane. Asterisk, autoradiograph background. Each lane contains SPO11–oligonucleotides from the equivalent of different numbers of mice in order to better compare sizes: $Atm^{+/+}$, 15 mice; $Atm^{-/-}$, 2 mice; $Spo11^{+/-}$ $Atm^{-/-}$, 4 mice; $Atm^{-/-}$ plus transgene, 2 mice; $Spo11^{-/-}$, 2 mice; mock, 15 wild-type mice. nt, nucleotides. **b**, Negative feedback loop by which ATM regulates meiotic DSB levels. DSBs generated by SPO11 activate the ATM kinase, inhibiting further DSB formation. ATM may also have roles in repair of DSBs by homologous recombination; for example, by promoting DSB end resection.

METHODS SUMMARY

Mouse mutant alleles and the *Spo11β* transgene were previously described[10,18,28–30]. Experimental animals were compared with controls from the same litter. Experiments conformed to regulatory standards and were approved by the MSKCC Institutional Animal Care and Use Committee. For measurement of SPO11–oligonucleotide complexes, both testes from each mouse were used per experiment, that is, littermate comparisons were made on a per-testis basis (Supplementary Fig. 1). Testis extract preparation, immunoprecipitation and western blot analysis were performed essentially as described[7]. Radiolabelled species were quantified with Fuji phosphor screens and ImageGuage software. The anti-mouse SPO11 monoclonal antibody was produced from hybridoma cell line 180 (M.P.T., unpublished data). The size distribution of SPO11–oligonucleotides was determined essentially as described[5] after radiolabelling with [α-^{32}P] cordycepin. Benzonase treatment of SPO11–oligonucleotide complexes followed manufacturer's instructions (Novagen).

Full Methods and any associated references are available in the online version of the paper at www.nature.com/nature.

Received 23 June; accepted 25 August 2011.
Published online 16 October 2011.

1. Keeney, S. in *Recombination and Meiosis: Crossing-Over and Disjunction* Vol. 2 (ed. Lankenau, D. H.) 81–123 (Springer, 2007).
2. Cole, F., Keeney, S. & Jasin, M. Evolutionary conservation of meiotic DSB proteins: more than just Spo11. *Genes Dev.* **24,** 1201–1207 (2010).
3. Sasaki, M., Lange, J. & Keeney, S. Genome destabilization by homologous recombination in the germ line. *Nature Rev. Mol. Cell Biol.* **11,** 182–195 (2010).
4. Hochwagen, A. & Amon, A. Checking your breaks: surveillance mechanisms of meiotic recombination. *Curr. Biol.* **16,** R217–R228 (2006).
5. Neale, M. J., Pan, J. & Keeney, S. Endonucleolytic processing of covalent protein-linked DNA double-strand breaks. *Nature* **436,** 1053–1057 (2005).
6. Pan, J. *et al.* A hierarchical combination of factors shapes the genome-wide topography of yeast meiotic recombination initiation. *Cell* **144,** 719–731 (2011).
7. Daniel, K. *et al.* Meiotic homologue alignment and its quality surveillance are controlled by mouse HORMAD1. *Nature Cell Biol.* **13,** 599–610 (2011).
8. Barlow, C. *et al.* Atm-deficient mice: a paradigm of ataxia telangiectasia. *Cell* **86,** 159–171 (1996).
9. Xu, Y. *et al.* Targeted disruption of ATM leads to growth retardation, chromosomal fragmentation during meiosis, immune defects, and thymic lymphoma. *Genes Dev.* **10,** 2411–2422 (1996).
10. Barlow, C. *et al.* Atm deficiency results in severe meiotic disruption as early as leptonema of prophase I. *Development* **125,** 4007–4017 (1998).
11. Di Giacomo, M. *et al.* Distinct DNA-damage-dependent and -independent responses drive the loss of oocytes in recombination-defective mouse mutants. *Proc. Natl Acad. Sci. USA* **102,** 737–742 (2005).
12. Barchi, M. *et al.* Surveillance of different recombination defects in mouse spermatocytes yields distinct responses despite elimination at an identical developmental stage. *Mol. Cell. Biol.* **25,** 7203–7215 (2005).
13. Bellani, M. A., Romanienko, P. J., Cairatti, D. A. & Camerini-Otero, R. D. SPO11 is required for sex-body formation, and Spo11 heterozygosity rescues the prophase arrest of $Atm^{-/-}$ spermatocytes. *J. Cell Sci.* **118,** 3233–3245 (2005).

14. Barchi, M. *et al.* ATM promotes the obligate XY crossover and both crossover control and chromosome axis integrity on autosomes. *PLoS Genet.* **4,** e1000076 (2008).
15. Keeney, S. *et al.* A mouse homolog of the *Saccharomyces cerevisiae* meiotic recombination DNA transesterase Spo11p. *Genomics* **61,** 170–182 (1999).
16. Shannon, M., Richardson, L., Christian, A., Handel, M. A. & Thelen, M. P. Differential gene expression of mammalian *SPO11/TOP6A* homologs during meiosis. *FEBS Lett.* **462,** 329–334 (1999).
17. Bellani, M. A., Boateng, K. A., McLeod, D. & Camerini-Otero, R. D. The expression profile of the major mouse SPO11 isoforms indicates that SPO11β introduces double strand breaks and suggests that SPO11α has an additional role in prophase in both spermatocytes and oocytes. *Mol. Cell. Biol.* **30,** 4391–4403 (2010).
18. Kauppi, L. *et al.* Distinct properties of the XY pseudoautosomal region crucial for male meiosis. *Science* **331,** 916–920 (2011).
19. Romanienko, P. J. & Camerini-Otero, R. D. Cloning, characterization, and localization of mouse and human *SPO11*. *Genomics* **61,** 156–169 (1999).
20. Romanienko, P. J. & Camerini-Otero, R. D. The mouse *Spo11* gene is required for meiotic chromosome synapsis. *Mol. Cell* **6,** 975–987 (2000).
21. Bellve, A. R. *et al.* Spermatogenic cells of the prepuberal mouse. Isolation and morphological characterization. *J. Cell Biol.* **74,** 68–85 (1977).
22. Eaker, S., Cobb, J., Pyle, A. & Handel, M. A. Meiotic prophase abnormalities and metaphase cell death in MLH1-deficient mouse spermatocytes: insights into regulation of spermatogenic progress. *Dev. Biol.* **249,** 85–95 (2002).
23. Terasawa, M., Ogawa, T., Tsukamoto, Y. & Ogawa, H. Sae2p phosphorylation is crucial for cooperation with Mre11p for resection of DNA double-strand break ends during meiotic recombination in *Saccharomyces cerevisiae*. *Genes Genet. Syst.* **83,** 209–217 (2008).
24. Sasanuma, H. *et al.* Cdc7-dependent phosphorylation of Mer2 facilitates initiation of yeast meiotic recombination. *Genes Dev.* **22,** 398–410 (2008).
25. Mahadevaiah, S. K. *et al.* Recombinational DNA double-strand breaks in mice precede synapsis. *Nature Genet.* **27,** 271–276 (2001).
26. Sedgwick, R. P. & Boder, E. in *Handbook of Clinical Neurology* Vol. 16 (ed. de Jong, J. M. B. V.) 347–423 (Elsevier, 1991).
27. Savitsky, K. *et al.* A single ataxia telangiectasia gene with a product similar to PI-3 kinase. *Science* **268,** 1749–1753 (1995).
28. Edelmann, W. *et al.* Meiotic pachytene arrest in MLH1-deficient mice. *Cell* **85,** 1125–1134 (1996).
29. Pittman, D. L. *et al.* Meiotic prophase arrest with failure of chromosome synapsis in mice deficient for *Dmc1*, a germline-specific RecA homolog. *Mol. Cell* **1,** 697–705 (1998).
30. Baudat, F., Manova, K., Yuen, J. P., Jasin, M. & Keeney, S. Chromosome synapsis defects and sexually dimorphic meiotic progression in mice lacking Spo11. *Mol. Cell* **6,** 989–998 (2000).

Supplementary Information is linked to the online version of the paper at www.nature.com/nature.

Acknowledgements We thank M. Neale for discussions, R. Cha and K. McKim for sharing data before publication, and M. Hwang for assistance in monoclonal antibody development. This work was supported by NIH grants HD040916 and HD053855 (to M.J. and S.K.) and GM058673 (to S.K.). J.P. was supported in part by a Leukemia and Lymphoma Society Fellowship and F.C. by a Ruth L. Kirschstein NRSA (F32 HD51392). S.K. is an Investigator of the Howard Hughes Medical Institute.

Author Contributions J.L., J.P. and F.C. performed experiments. M.P.T. generated the anti-SPO11 monoclonal hybridoma line. J.L., M.J., and S.K. wrote the paper.

Author Information Reprints and permissions information is available at www.nature.com/reprints. The authors declare no competing financial interests. Readers are welcome to comment on the online version of this article at www.nature.com/nature. Correspondence and requests for materials should be addressed to S.K. (s-keeney@ski.mskcc.org) or M.J. (m-jasin@ski.mskcc.org).

METHODS

Mouse mutant alleles and the *Spo11β* transgene were previously described[10,18,28–30]. Experiments conformed to regulatory standards and were approved by the MSKCC Institutional Animal Care and Use Committee. For measurement of SPO11–oligonucleotide complexes, both testes from each mouse were used per experiment, that is, littermate comparisons were made on a per-testis basis (Supplementary Fig. 1). The anti-mouse SPO11 monoclonal antibody was produced from hybridoma cell line 180 (M.P.T., unpublished data).

Testis extract preparation, immunoprecipitation and western blot analysis were performed essentially as described[7]. Testes were decapsulated, then lysed in 800 µl lysis buffer (1% Triton X-100, 400 mM NaCl, 25 mM HEPES-NaOH at pH 7.4, 5 mM EDTA). Lysates were centrifuged at 100,000 r.p.m. (355,040*g*) for 25 min in a TLA100.2 rotor. Supernatants were incubated with anti-mouse SPO11 antibody 180 (5 µg per pair of testes) at 4 °C for 1 h, followed by addition of 30–40 µl protein-A–agarose beads (Roche) and incubation for another 3 h. Beads were washed three times with IP buffer (1% Triton X-100, 150 mM NaCl, 15 mM Tris-HCl at pH 8.0). Immunoprecipitates were eluted with Laemmli sample buffer and diluted six- to sevenfold in IP buffer. Eluates were incubated with additional anti-mouse SPO11 antibody 180 at 4 °C for 1 h, followed by addition of 30–40 µl protein-A–agarose beads and incubation at 4 °C overnight. Beads were washed three times with IP buffer and twice with buffer NEB4 (New England BioLabs). SPO11–oligonucleotide complexes were radiolabelled at 37 °C for 1 h using terminal deoxynucleotidyl transferase (Fermentas) and [α-^{32}P] dCTP. Beads were washed three times with IP buffer, boiled in Laemmli sample buffer and fractionated on 8% SDS–PAGE. Complexes were transferred to a PVDF membrane by semi-dry transfer (Bio-Rad). Radiolabelled species were detected and quantified with Fuji phosphor screens and ImageGuage software. For western blot analysis, membranes were probed with anti-mouse SPO11 antibody 180 (1:2,000 in PBS containing 0.1% Tween 20 and 5% non-fat dry milk), then horseradish-peroxidase-conjugated protein A (Abcam; 1:10,000 in PBS containing 0.1% Tween 20 and 5% non-fat dry milk), and detected using the ECL+ reagent (GE Healthcare). The size distribution of SPO11–oligonucleotides was determined by radiolabelling with [α-^{32}P] cordycepin then protease digestion followed by denaturing PAGE. Benzonase treatment of SPO11–oligonucleotide complexes was performed as per manufacturer's instructions (Novagen).